

Unveiling New Magnetic Phases of Undoped and Doped Manganites

Takashi Hotta¹, Mohammad Moraghebi², Adrian Feiguin³, Adriana Moreo², Seiji Yunoki⁴, and Elbio Dagotto²

¹Advanced Science Research Center, Japan Atomic Energy Research Institute, Tokai, Ibaraki 319-1195, Japan

²National High Magnetic Field Laboratory, Florida State University, Tallahassee, Florida 32306

³Department of Physics and Astronomy, University of California at Irvine, CA 92697

⁴International School for Advanced Studies (SISSA), via Beirut 4, 34014 Trieste, Italy

(Dated: September 2, 2002)

Novel ground-state spin structures in undoped and doped manganites are here investigated based on the orbital-degenerate double-exchange model, by using mean-field and numerical techniques. In undoped manganites, a new antiferromagnetic (AFM) state, called the E-type phase, is found adjacent in parameter space to the A-type AFM phase. Its structure is in agreement with recent experimental results. This insulating E-AFM state is competing with a ferromagnetic metallic phase as well, suggesting that large magneto-resistant effects could exist even in undoped manganese oxides. For doped layered manganites, the phase diagram includes another new AFM phase of the C_xE_{1-x} -type. Experimental signatures of the new phases are discussed.

PACS numbers: PACS numbers: 75.30.Vn, 75.30.Kz, 75.50.Ee, 75.10.-b

In the recent decade, the study of manganites – materials that show a remarkable Colossal Magneto-Resistance (CMR) [1] – has been one of the most important areas of research in condensed matter physics [2]. This CMR effect can be understood if the manganite ground-state changes from insulating to ferromagnetic (FM) metallic by a small magnetic field. Based on the concept of two-phase competition [2], the CMR behavior has been successfully qualitatively reproduced in computational simulations employing resistor network models [3]. However, more work remains to be done to fully understand Mn-oxides, both regarding their unusual magneto-transport properties and the nature of the many competing phases.

The appearance of the FM metallic phase in manganites is usually rationalized by the so-called double-exchange (DE) mechanism, based on a strong Hund coupling between mobile e_g electrons and localized t_{2g} spins. On the other hand, the insulating phase in manganites occurs due to the coupling between degenerate e_g electrons and Jahn-Teller (JT) distortions of the MnO_6 octahedra, leading to the various types of charge and/or orbital orders observed experimentally [2].

The parent compound of CMR manganites is undoped $RMnO_3$, where R denotes rare earth lanthanide ions. For R=La, it is well known that the A-type antiferromagnetic (AFM) phase appears, with the C-type ordering of the $(3x^2-r^2)$ - and $(3y^2-r^2)$ -orbitals [4]. By substituting La by alkaline earth ions such as Sr and Ca, holes are doped into the e_g -electron band and due to the DE mechanism, the FM metallic phase appears, with its concomitant CMR effect. Most of the discussion in manganites has centered on the many phases induced by doping with holes the A-type AFM state, at different values of their bandwidths. In this framework, it is implicitly assumed that the undoped material is always in an A-type state. However, quite recently, a new AFM phase was reported as the ground-state in the undoped limit for R=Ho [5, 6]. This phase is here called the “E-type” spin structure for reasons to be explained below [7]. It is surprising that

a new phase can be still found even in the undoped material, previously considered to be well understood. In addition, the nature of the states obtained by doping this E-phase is totally unknown, and new phenomena may be unveiled experimentally in the near future. Overall, this opens an exciting new branch of investigations in manganites since novel phases appear to be hidden in the vast parameter space of these compounds.

In this Letter, based on the orbital-degenerate DE model coupled with JT distortions, the ground state properties of undoped manganites are analyzed by using mean-field (MF) calculations and Monte-Carlo (MC) simulations. In our phase diagram at $x=0$, the E-AFM phase was found to exist in a *wide* region of parameter space, adjacent to the A-AFM phase in agreement with the experimental results. The E-AFM phase is robust when the dimensionality and/or electron-phonon coupling are modified, and it will be argued that its strength originates in the intrinsic nature of orbital-degenerate DE systems. In the phase diagram and at small electron-phonon coupling the E-AFM insulating phase is located just next to a FM metallic phase, suggesting that the CMR effect could be found even at $x=0$. Hole doping x of the E-type phase is also discussed and another novel magnetic phase, defined as the “ C_xE_{1-x} ” phase, is found. The ubiquitous phase-separation tendencies observed when insulating and metallic phases compete is also expected near the FM- C_xE_{1-x} boundary.

The Hamiltonian studied in this paper is

$$\begin{aligned}
 H = & - \sum_{\mathbf{i}\alpha\gamma\gamma'\sigma} t_{\gamma\gamma'}^{\mathbf{a}} d_{\mathbf{i}\gamma\sigma}^\dagger d_{\mathbf{i}+\mathbf{a}\gamma'\sigma} - J_H \sum_{\mathbf{i}} \mathbf{s}_{\mathbf{i}} \cdot \mathbf{S}_{\mathbf{j}} \\
 & + J_{AF} \sum_{\langle \mathbf{i}, \mathbf{j} \rangle} \mathbf{S}_{\mathbf{i}} \cdot \mathbf{S}_{\mathbf{j}} + \lambda \sum_{\mathbf{i}} (Q_{1i}\rho_i + Q_{2i}\tau_{xi} + Q_{3i}\tau_{zi}) \\
 & + (1/2) \sum_{\mathbf{i}} (\beta Q_{1i}^2 + Q_{2i}^2 + Q_{3i}^2),
 \end{aligned} \tag{1}$$

where $d_{i\alpha\sigma}$ ($d_{i\beta\sigma}$) annihilates an e_g -electron with spin σ in the $d_{x^2-y^2}$ ($d_{3z^2-r^2}$) orbital at site \mathbf{i} , and \mathbf{a} is

the vector connecting nearest-neighbor (NN) sites. The first term is the NN hopping of e_g electrons with amplitude $t_{\gamma\gamma}^{\mathbf{a}}$ between γ - and γ' -orbitals along the \mathbf{a} -direction, where $t_{aa}^{\mathbf{x}} = -\sqrt{3}t_{ab}^{\mathbf{x}} = -\sqrt{3}t_{ba}^{\mathbf{x}} = 3t_{bb}^{\mathbf{x}} = t$ for $\mathbf{a}=\mathbf{x}$, $t_{aa}^{\mathbf{y}} = \sqrt{3}t_{ab}^{\mathbf{y}} = \sqrt{3}t_{ba}^{\mathbf{y}} = 3t_{bb}^{\mathbf{y}} = t$ for $\mathbf{a}=\mathbf{y}$, and $t_{aa}^{\mathbf{z}} = t_{ab}^{\mathbf{z}} = t_{ba}^{\mathbf{z}} = 0$ for $\mathbf{a}=\mathbf{z}$, respectively. Hereafter, t is taken as the energy unit. In the second term, the Hund coupling $J_H(>0)$ links e_g electrons with spin $\mathbf{s}_i = \sum_{\gamma\alpha\beta} d_{i\gamma\alpha}^\dagger \sigma_{\alpha\beta} d_{i\gamma\beta}$ (σ = Pauli matrices) with the localized t_{2g} spin \mathbf{S}_i , assumed classical with $|\mathbf{S}_i|=1$. J_H is here considered as infinite or very large. The third term is the AFM coupling J_{AF} between NN t_{2g} spins. The fourth term couples e_g electrons and MnO_6 octahedra distortions, λ is a dimensionless coupling constant, Q_{1i} is the breathing-mode distortion, Q_{2i} and Q_{3i} are, respectively, (x^2-y^2) - and $(3z^2-r^2)$ -type JT-mode distortions, $\rho_i = \sum_{\gamma\sigma} d_{i\gamma\sigma}^\dagger d_{i\gamma\sigma}$, $\tau_{xi} = \sum_{\sigma} (d_{ia\sigma}^\dagger d_{ib\sigma} + d_{ib\sigma}^\dagger d_{ia\sigma})$, and $\tau_{zi} = \sum_{\sigma} (d_{ia\sigma}^\dagger d_{ia\sigma} - d_{ib\sigma}^\dagger d_{ib\sigma})$. The fifth term is the usual quadratic potential for distortions, and β is the ratio of spring constants for breathing- and JT-modes [8], treated here adiabatically.

In undoped manganites, all oxygens are shared by adjacent MnO_6 octahedra and the distortions are not independent, suggesting that the cooperative effect is even more important than for the doped case $x>0$. To consider this cooperation, the simplest way is to optimize directly the oxygen ions displacement. In practice, considering sites \mathbf{i} and $\mathbf{i}+\mathbf{a}$, the oxygen in between is here only allowed to move along the \mathbf{a} -axis (buckling and rotations are neglected). In this paper, the apical oxygens in the two-dimensional (2D) case are assumed to be static, consistent with previous treatments to produce stripe-like charge ordering in the 2D FM-phase [9].

Let us first describe our results in 2D, since the essential physics behind the stabilization of the E-type phase can be grasped by using MC simulations with relatively short CPU times. The phase diagram on a 4×4 lattice is shown in Fig. 1(a). The continuous curves are obtained by comparing the energies of the competing phases in the MF calculations, while the circles are obtained by monitoring the nature of the dominant spin correlation $S(\mathbf{q})$ in MC simulations. A typical result for $S(\mathbf{q})$ is shown in Fig. 1(b). A new regime characterized by $\mathbf{q}=(\pi/2, \pi/2)$ is clearly observed between the previously known FM – with peak at $(0, 0)$ – and G-AFM –peak at (π, π) – limits. Clearly, there is a good agreement between MF and MC results in the region of interest, showing the high accuracy of the present MF calculations for CMR manganites, as emphasized previously [10].

In Fig. 1(c), the spin and orbital structure of the novel intermediate phase (E-phase) is shown. Along the zigzag chains, the t_{2g} spins order ferromagnetically, but they are antiparallel perpendicular to the zigzag direction. In three dimensions, the MF study shows that the pattern Fig. 1(c) just *stacks* along the z -axis, while the spin directions are reversed from plane to plane. Note also that the orbital structure is the same as that of the A-AFM

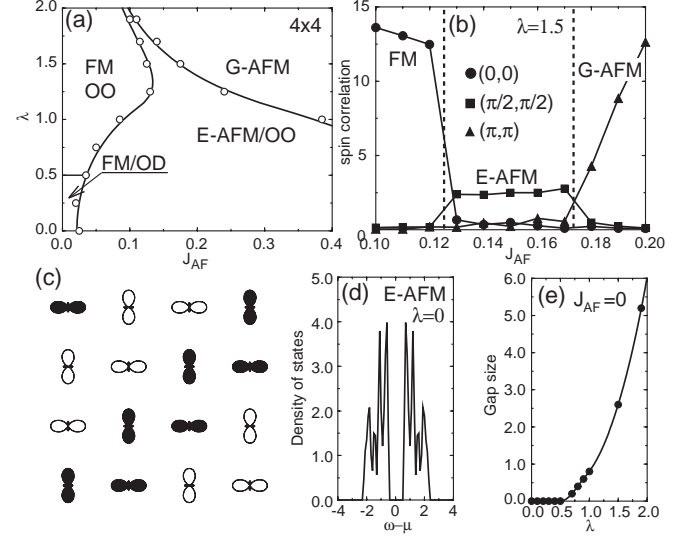


FIG. 1: (a) Phase diagram obtained using the 4×4 lattice. Open circles denote MC results and solid lines are obtained with MF calculations. (b) Spin correlations vs. J_{AF} at $\lambda=1.5$. (c) Schematic view of the spin and orbital structure of the E-AFM phase. Solid and open symbols denote orbitals with up- and down-spins, respectively. Note the presence of zigzag chains for each spin orientation. (d) Density of states (DOS) of the E-phase obtained by MC simulations at $\lambda=0$. (e) Gap at the Fermi level for the FM phase vs. λ . The gap magnitude is evaluated from the DOS obtained by MC simulations.

phase, namely, the staggered pattern of $(3x^2-r^2)$ - and $(3y^2-r^2)$ -like orbitals [4]. Our investigations show that the E-phase is robust at weak- and intermediate- λ , but for $\lambda>1.5$, the E-type regime narrows.

A surprising aspect of our results is that the E-type spin arrangement is the ground-state for a *wide* range of J_{AF} , even at $\lambda=0$, indicating that the coupling with JT phonons is *not* a necessary condition for its stabilization. This is in sharp contrast to the case of the A-AFM phase. To understand this point, it is instructive to study the e_g -electronic structure of the zigzag FM chains that appear in the E-phase spin arrangement. Taking J_H as infinity for simplicity, the e_g electrons move only along the zigzag FM chain, and cannot hop to the adjacent FM chains. The dispersion energy for e_g electrons in this zigzag FM chain is given by $\varepsilon_k = (2/3)(\cos k \pm \sqrt{\cos^2 k + 3})$ and $(2/3)(-\cos k \pm \sqrt{\cos^2 k + 3})$, indicating that there appears a large *band-gap* equal to $4t/3$ at half-filling. In fact, as shown in Fig. 1(d), even on the 4×4 cluster, there is a clear gap of the order of t for the E-phase. Since $t_{\mu\nu}^{\mathbf{x}} = -t_{\mu\nu}^{\mathbf{y}}$ for $\mu \neq \nu$, the sign in the hopping amplitude changes periodically in the zigzag situation, leading to a periodic potential for the e_g electrons, and its concomitant band-insulator nature at $x=0$. In other words, the E-type phase is stable due to the zigzag *geometry* of the FM chains that induce a band-insulator [11].

Another related interesting point is the orbital structure of the FM phase. In the strong-coupling region, an

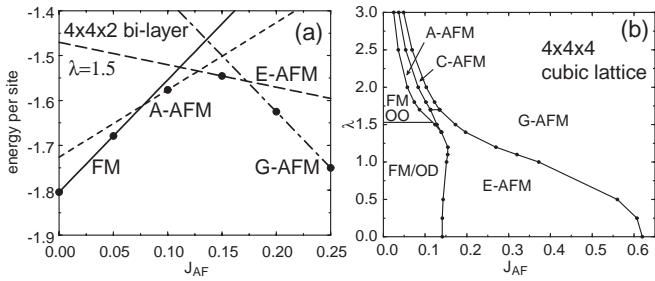


FIG. 2: (a) Energies of the FM, A-AFM, E-AFM, C-AFM, and G-AFM phases on $4 \times 4 \times 2$ bi-layer lattices ($\lambda=1.5$). Solid circles indicate the results of optimizations, while lines denote the MF results. (b) Phase diagram for the $4 \times 4 \times 4$ cubic lattice. All solid lines emerge from MF calculations.

orbitally ordered (OO) state appears, essentially with the same pattern as that observed in the E-AFM phase discussed above. For $n=1$ ($n=1-x$ is the e_g electron number per site), all MnO_6 octahedra are distorted and the cooperative effect is essential to determine the OO pattern for large λ , irrespective of the spin structure. However, when λ decreases OO *disappears* and an orbital disordered (OD) new phase is observed. The OO-OD transition is monitored by the gap size at the Fermi level in the DOS (Fig. 1(e)). Note that the transition observed using a 4×4 cluster is robust, although the actual critical value may change in larger systems. By analytic calculations (to be discussed elsewhere) it has been confirmed that the metal-insulator transition driven by JT phonons occurs at a *finite* value of λ in the infinite lattice. Note also that the E-phase is always insulating, with a DOS gap both at small and large λ .

Here it should be noted that the metallic OD/FM phase is next to the insulating E-AFM phase for $\lambda \lesssim 0.5$. Such a result is new in the study of undoped manganites, since only properties in the strong coupling region have been considered to be important before [4]. As emphasized in the introduction, the competition between FM metallic and insulating phases is at the heart of the CMR phenomena. Thus, by tuning experimentally the lattice parameters in $RMnO_3$, it may be possible to observe the CMR behavior and the magnetic-field induced metal-insulator transition *even in undoped manganites without hole doping*. It is interesting to investigate the CMR phenomena using an undoped material, since hole doping inevitably introduces quenched disorder adding more complexity to the problem.

Consider now the effect of dimensionality. In Fig. 2(a), using bi-layer $4 \times 4 \times 2$ clusters, the ground state energy per site is depicted vs. J_{AF} at $\lambda=1.5$ both for numerical optimization [12] and MF calculations, with a good agreement between them. Figure 2(b) is the phase diagram on a $4 \times 4 \times 4$ cubic lattice, obtained only by the MF approximation since MC calculations in this case are too CPU time consuming (previous MF-MC comparisons suggest that this MF phase diagram is accurate). In the strong-coupling region, there occurs a

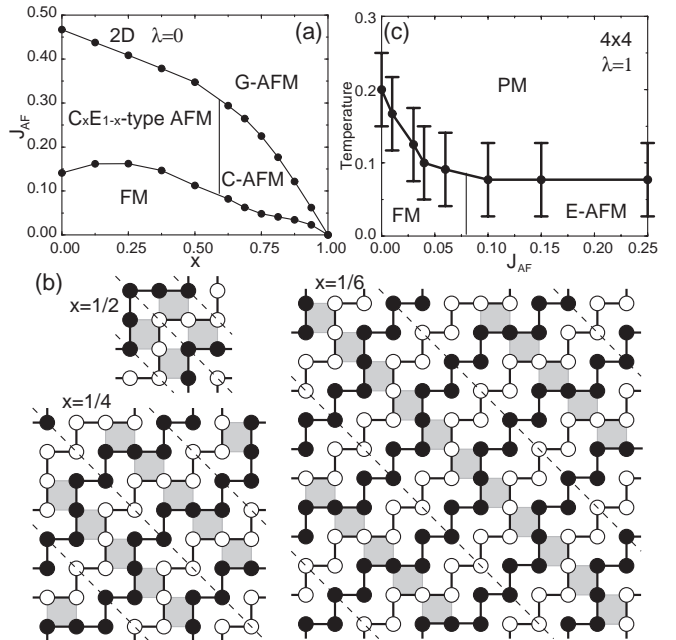


FIG. 3: (a) Phase diagram in the (x, J_{AF}) plane for layered manganites at $\lambda=0$ obtained by analytic calculations. (b) Schematic view of the C_xE_{1-x} -type phase at $x=1/2, 1/4$, and $1/6$. Open and solid circles indicate up- and down-spins, respectively. Hatched squares denote C-type regions. Dashed lines indicate the hole positions in the strong-coupling limit. (c) Phase diagram in the (J_{AF}, T) plane at $x=0$ and $\lambda=1$, using a 4×4 lattice. Estimations of the Curie and Néel temperatures are evaluated using MC simulations, from the behavior of the spin correlations (see text).

chain of transitions from $FM \rightarrow A\text{-AFM} \rightarrow C\text{-AFM} \rightarrow G\text{-AFM}$ phases [13], already obtained in $2 \times 2 \times 2$ calculations [4]. The present result shows that size effect are small in undoped strongly-coupled manganites, which is intuitively reasonable. Note that near $\lambda \sim 1.6$, a realistic value for manganites, the A-AFM phase is adjacent to the E-type state. This region could correspond to the actual situation observed in experiments for $RMnO_3$: When the ionic radius of the R-site decreases, the Néel temperature T_N of the A-AFM phase decreases as well, and eventually the E-AFM phase is stabilized for $R=Ho$ [6]. In the weak-coupling region, the E-type phase is stable in a wide range of J_{AF} , as in the 2D calculation. This robustness of the E-type phase at small λ indicates again that its stability must originate in intrinsic properties of orbital degenerate DE system.

Let us now consider the very interesting effect of hole doping on the E-phase. Hole doping will be here studied in the weak coupling limit, since the E-type phase is well understood at $\lambda=0$. Figure 3(a) shows the ground-state phase diagram in the (x, J_{AF}) plane, obtained using analytic calculations on 2D lattices at $\lambda=0$. A remarkable feature of this phase diagram is the appearance of the novel C_xE_{1-x} phase, composed of long-period zigzag FM chains, which are antiferromagnetically coupled to each

other (see Fig. 3(b) for $x=1/4$ and $1/6$). Note that at $x=1/2$, the well-known CE-type phase appears [14].

Note that the curvature of the boundary curve between FM and C_xE_{1-x} phases was found to be *negative* for $0 \lesssim x \lesssim 0.5$, indicating that phase separation occurs around the boundary between those two phases. Here it is again stressed that the FM phase is metallic, while C_xE_{1-x} is insulating. The latter can be considered as a microscopic phase separated state, since the C- and E-type structure are mixed at the length scale of a lattice constant. This phase is expected to be made unstable easily near the phase boundary region, and to turn into a phase-separated state with a mixture of metallic FM and insulating C_xE_{1-x} clusters, which may induce CMR effects.

For $x < 0.5$ with large λ , the C_xE_{1-x} -AFM phase has been found to exist for $x=1/3$ and $1/4$ using numerical techniques [9, 15], but its importance at other densities and couplings was not discussed. For $x=1/6$ with the spin structure shown in Fig. 3(b), e_g electrons tend to localize in the C-type region, i.e., in the straight segment portion of the zigzag FM chain, as in the CE-type phase at $x=1/2$ [14]. Namely, holes localize to form *stripes* just in the center between charged C-type regions, as shown by dashed lines in Fig. 3(b), leading to incommensurate peaks in the charge correlation at $\mathbf{q}=(2\pi x, 2\pi)$.

On the other hand, for $x > 0.5$ in the strong-coupling case, the position of the C_xE_{1-x} and C-AFM phases boundary may be shifted. Note that the C_xE_{1-x} -phase is compatible with the so-called Wigner-crystal charge-orbital ordered structure suggested for $x=2/3$ and $3/4$ in $La_{1-x}Ca_xMnO_3$ [16]. However, the bi-stripe charge-orbital ordered phase suggested by Mori *et al.* [17] is consistent with the $C_{1-x}E_x$ -AFM state [14], which emerges from the competition with the Wigner-crystal structure [18]. Experimentally, the C_xE_{1-x} -AFM phase was reported for $x > 0.5$ in $Nd_{1-x}Sr_{1+x}MnO_4$ [19].

Finally, let us discuss the effect of thermal fluctuations.

For this purpose, both T_C (Curie temperature) and T_N were estimated from our MC simulations using 4×4 clusters, as shown in Fig. 3(c). While finite clusters do not show true thermodynamic singularities, a rapid increase in the strength of correlations was observed at fairly well defined temperatures, here referred to as T_N and T_C for simplicity. Previous computational experience [2] shows that these estimations are fairly accurate upon increasing lattice sizes. Our estimated T_C is found to decrease with increasing J_{AF} , and in the E-AFM phase, T_N becomes almost constant. The E-phase can be disordered by thermal fluctuations faster upon heating than the FM phase. Provided that our estimated T_C in 2D system is related to T_N with the A-AFM phase of 3D lattices, Fig. 3(c) mimics well the experimental results for the changes of T_N , when rare earth ions are substituted in $RMnO_3$ [6].

In summary, the extended phase diagrams of manganites for $x=0$ and $x > 0$ have been discussed. A novel E-AFM phase, stabilized at $x=0$ in the region of weak- and intermediate-couplings, is adjacent to both FM metallic and A-AFM states. The competition between E-AFM insulating and FM metallic phases suggests the possibility of CMR effects even in undoped manganites. Several features of the E- to A-AFM transition, at least at the qualitative level, agrees with currently available experimental results. For the doped case, a microscopically inhomogeneous C_xE_{1-x} -AFM state is predicted. This state may contribute to the phase separation tendencies widely observed experimentally in Mn-oxides for $0 \lesssim x \lesssim 0.5$. Clearly, manganites have “hidden” interesting phases whose study is just starting.

The authors thank T. Kimura and K. Ueda for discussions. T.H. has been supported by a Grant-in-Aid for Scientific Research from the Ministry of Education, Culture, Sports, Science, and Technology of Japan. E. D. is supported by the NSF grant DMR-0122523.

[1] See, for instance, *Colossal Magnetoresistance Oxides*, edited by Y. Tokura, Gordon & Breach, New York, 2000.

[2] E. Dagotto *et al.*, Phys. Rep. **344**, 1 (2001). See also E. Dagotto, *Nanoscale Phase Separation and Colossal Magnetoresistance*, Springer-Verlag, Berlin, 2002.

[3] M. Mayr *et al.*, Phys. Rev. Lett. **86**, 135 (2001); J. Burgi *et al.*, Phys. Rev. Lett. **87**, 277202 (2001).

[4] T. Hotta *et al.*, Phys. Rev. B**60**, R15009 (1999) and references for $LaMnO_3$ therein.

[5] A. Muñoz *et al.*, Inorg. Chem. **40**, 1020 (2001).

[6] T. Kimura, S. Ishihara, K. T. Takahashi, S. Shintani, and Y. Tokura, in preparation.

[7] The conventions for “A” and “E” labeling to represent spin structures are defined in E. O. Wollan and W. C. Koehler, Phys. Rev. **100**, 545 (1955).

[8] In actual manganites with $\beta \approx 2$, breathing mode phonons are suppressed [4]. Thus, the results are not changed if β is set as infinity for simplicity.

[9] T. Hotta *et al.*, Phys. Rev. Lett. **86**, 4922 (2001).

[10] T. Hotta *et al.*, Phys. Rev. B**62**, 9432 (2000).

[11] A similar mechanism has been discussed by some of the authors for the CE-type phase at $x=0.5$ [14].

[12] Both spin directions and oxygen positions are optimized.

[13] Note that the FM/OO state of Fig. 2(b) is another phase not previously observed experimentally, here predicted to exist for low- J_{AF} manganites at $x=0$.

[14] T. Hotta *et al.*, Phys. Rev. Lett. **84**, 2477 (2000); S. Yunoki *et al.*, Phys. Rev. Lett. **84**, 3714 (2000).

[15] In 3D, the situation is more complicated, since another competition with a “pseudo” CE-type structure occurs, as shown in T. Hotta and E. Dagotto, Phys. Rev. B**61**, R11879 (2000).

[16] P. G. Radaelli *et al.*, Phys. Rev. B**59**, 14440 (1999); M. T. Fernández-Díaz *et al.*, Phys. Rev. B**59**, 1277 (1999).

[17] S. Mori *et al.*, Nature **392**, 473 (1998).

[18] T. Hotta *et al.*, Int. J. Mod. Phys. B**12**, 3437 (1998).

[19] T. Kimura *et al.*, Phys. Rev. B**65**, 020407(R) (2001).